COLLÈGE
DE FRANCE
1530

Collège de France abroad Lectures

Quantum information with real or artificial atoms and photons in cavities

Lecture 6:

Circuit QED experiments synthesing arbitrary states of quantum oscillators.

Introduction to State synthesis and reconstruction in Circuit QED

We describe in this last lecture Circuit QED experiments in which quantum harmonic oscillator states are manipulated and non-classical states are synthesised and reconstructed by coupling rf resonators to superconducting qubits. We start by the description of deterministic Fock state preparation (&VI-A), and we then generalize to the synthesis of arbitrary resonator states (§VI-B).

We finally describe an experiment in which entangled states of fields pertaining to two rf resonators have been generated and reconstructed (§VI-C). We compare these experiments to Cavity QED and ion trap studies.

VI-A

Deterministic preparation of Fock states in Circuit QED

*M.Hofheinz et al, Nature **454**, 310 (2008)*

Generating Fock states in a superconducting resonator

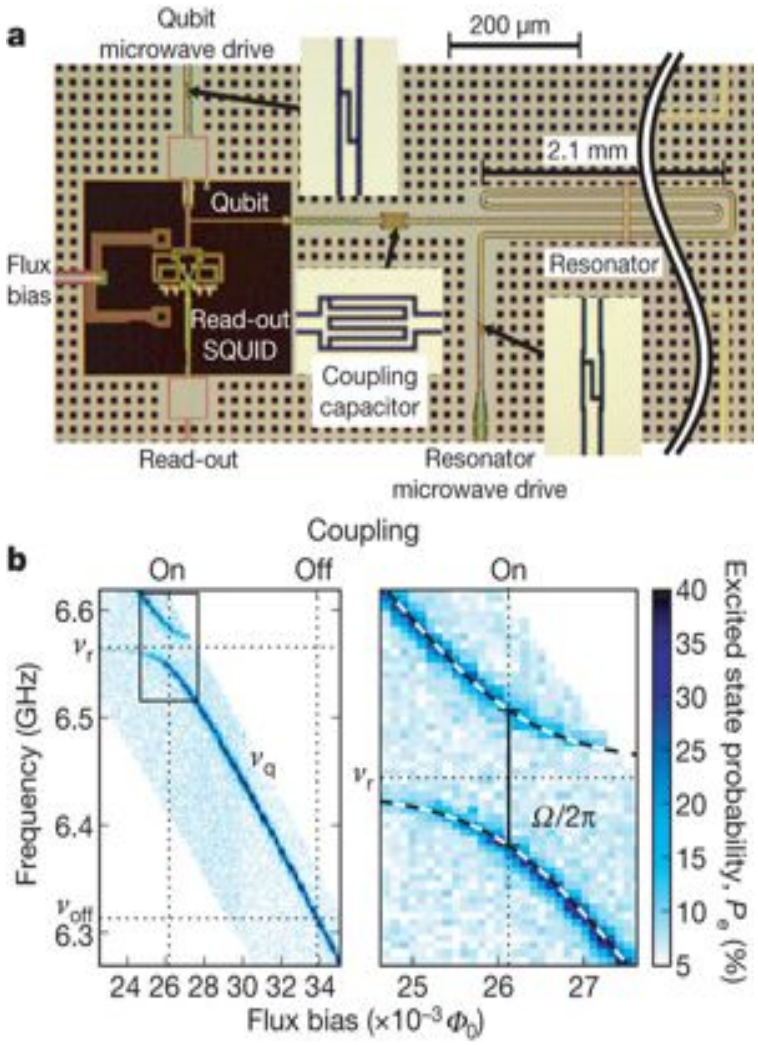

Microphotograph showing the phase qubit (left) and the coplanar resonator at 6.56 GHz (right) coupled by a capacitor. The qubit and the resonator are separately coupled to their own rf source. The phase qubit is tuned around the resonator frequency by using the flux bias. Qubit detection is achieved by a SQUID.

Figure montrant avec un code couleur (code sur l'échelle de droite) la probabilité de mesurer le qubit dans son état excité en fonction de la fréquence d'excitation (en ordonnée) et du désaccord du qubit par rapport au résonateur (en abscisse). Le spectre micro-onde obtenu montre l'anticroisement à résonance, la distance minimale des niveaux mesurant la fréquence de Rabi du vide $\Omega/2\pi$= 36 MHz.

*M.Hofheinz et al, Nature **454**, 310 (2008)*

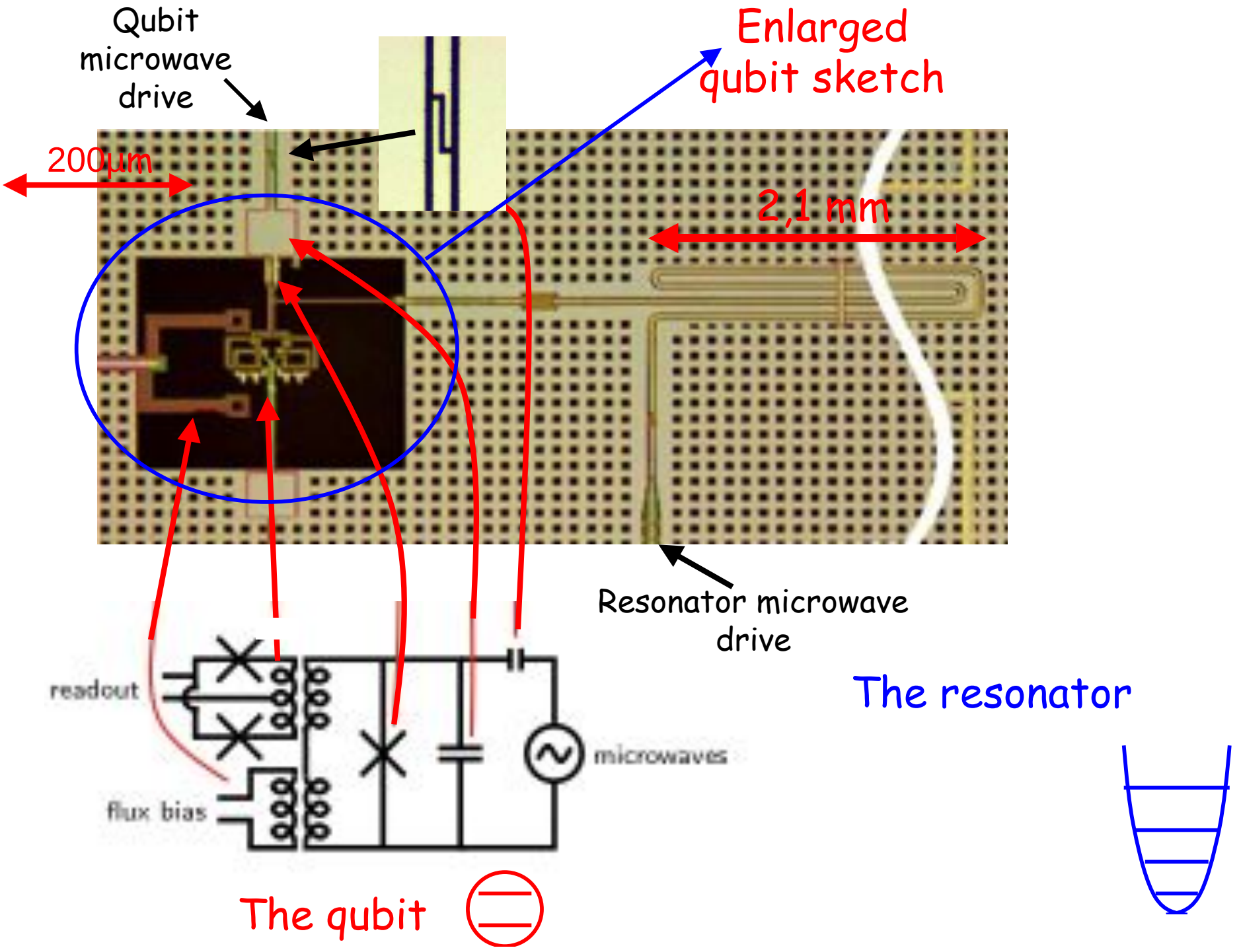
Qubit microwave drive
Enlarged qubit sketch
200µm
2,1 mm
Resonator microwave drive
readout
microwaves
flux bias
The qubit
The resonator

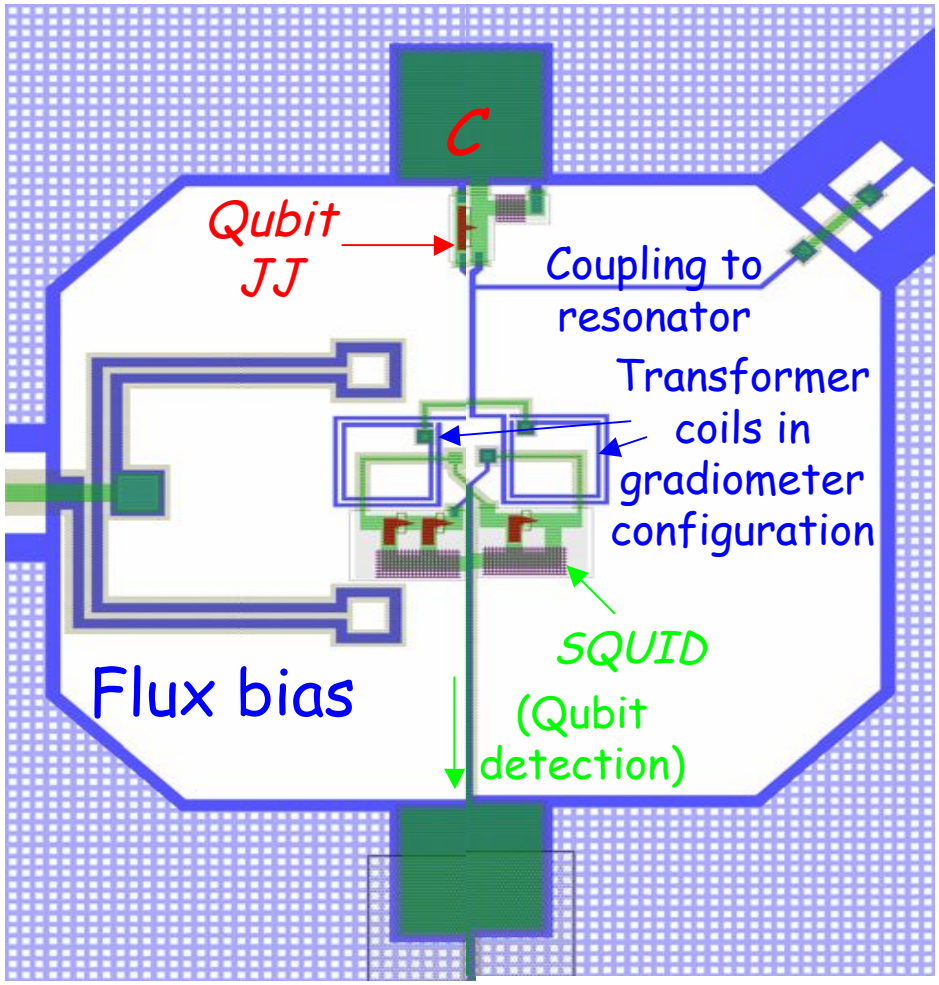
C
Qubit
JJ
Coupling to
resonator
Transformer
coils in
gradiometer
configuration
SQUID
(Qubit
detection)
Flux bias

Generating Fock states in a superconducting resonator

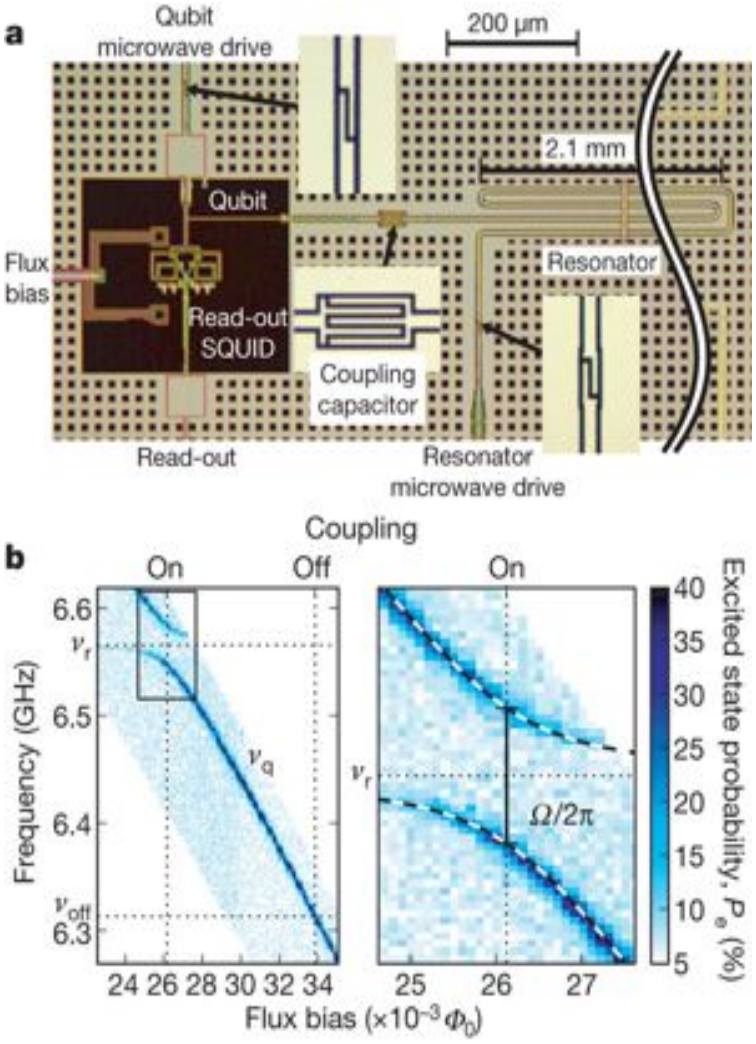

Microphotograph showing the phase qubit (left) and the coplanar resonator at 6.56 GHz (right) coupled by a capacitor. The qubit and the resonator are separately coupled to their own rf source. The phase qubit is tuned around the resonator frequency by using the flux bias. Qubit detection is achieved by a SQUID.

Figure showing with a color code (color scale at right) the probability for finding the qubit in its excited state versus its excitation frequency (vertical axis) and versus the resonator-qubit frequency mismatch (horizontal axis). The resulting microwave spectrum exhibits an anticrossing at resonance, the levels minimal distance measuring the vacuum Rabi frequency $\Omega/2\pi$ = 36 MHz.

M.Hofheinz et al, Nature ***454****, 310 (2008)*

Preparing and detecting the Fock states

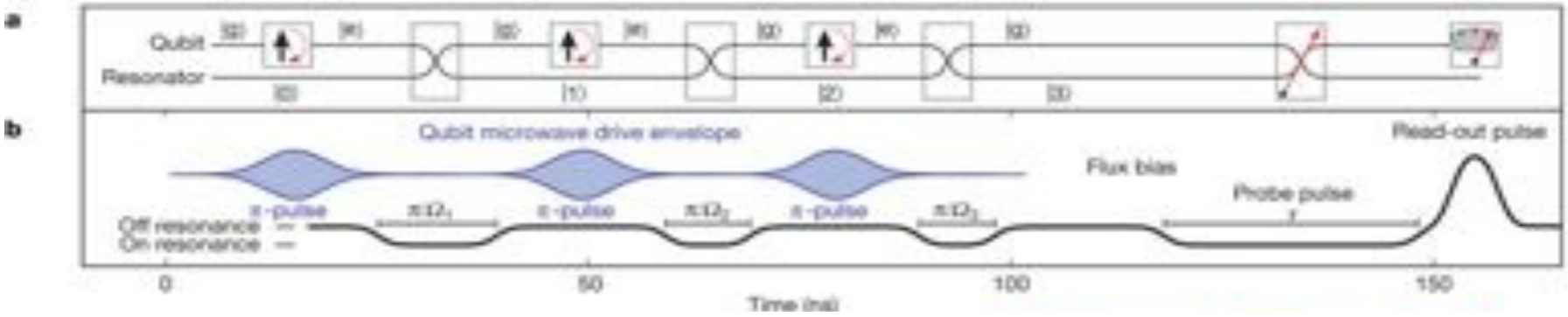

Sequence of operations introducing photons one by one in the resonator: The qubit (Q)-resonator (R) system is initialized in state $|g,0\rangle$. Q is then detuned from R and a π rf pulse is applied, bringing it into e. The Q-R system is then tuned into resonance during a time $\pi/\Omega_1 = \pi/\Omega$, resulting in energy exchange between Q and R according to the transformation $|e,0\rangle \rightarrow |g,1\rangle$. Q and R are then detuned again and a second π rf pulse resets Q in e. Q and R are then made resonant again during time $\pi/\Omega_2 = \pi/\Omega\sqrt{2}$, realizing the transformation $|e,1\rangle \rightarrow |g,2\rangle$…. And son on in order to inject 3, 4 …n photons in R. Once the Fock state $|n\rangle$ has been prepared, R is put again in resonance with Q during a variable time τ (probe pulse) before finally detecting the qubit in state e. The experiment is resumed many times for each value of τ to reconstruct $P_e(\tau)$. For a given n, $P_e(\tau)$ is expected to be a damped sine function with frequency $(\Omega\sqrt{n})/2\pi$.

Rabi Oscillation in a Fock state

The figure at left shows the Rabi oscillation in fields containing from 1 to 6 photons. The frequency increase scaling as √n is conspicuous. The figure at right shows with a color code the Fourier spectrum of the oscillating signal for the 6 n values. The main frequency component is found on a parabolic curve, thus quantitatively demonstrating the √n variation of the Rabi frequency. This experiment shows that the procedures of circuit QED are well-suited for the deterministic preparation of arbitrary Fock state. The maximum attainable n depends on decoherence: the preparation sequence must be applied faster than the state decays (see below).

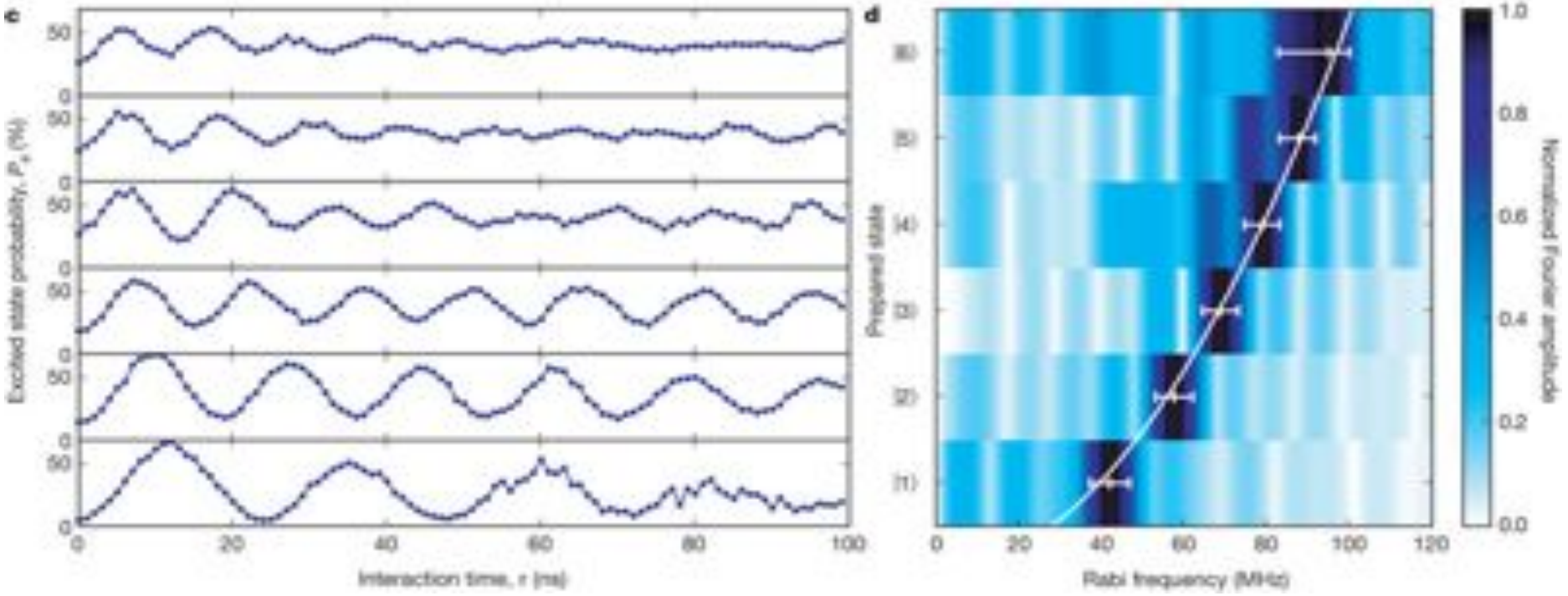

Rabi oscillation in a coherent state: « collapse and revivals »

A coherent state with amplitude α is prepared in R while Q is out of resonance in state g. Q and R are then tuned into resonance during a variable time τ , before detecting state e (procedure schematized in figs a and b).Statistics are accumulated as in the Fock state experiment. Fig.c shows the Rabi signals recorded with field amplitudes increasing from bottom to top. We observe the beating between the Rabi frequencies scaling as $\sqrt{n}$, each frequency corresponding to one of the Fock state in the superposition of each coherent state. The collapse and revival of the Rabi oscillation is clearly observed.

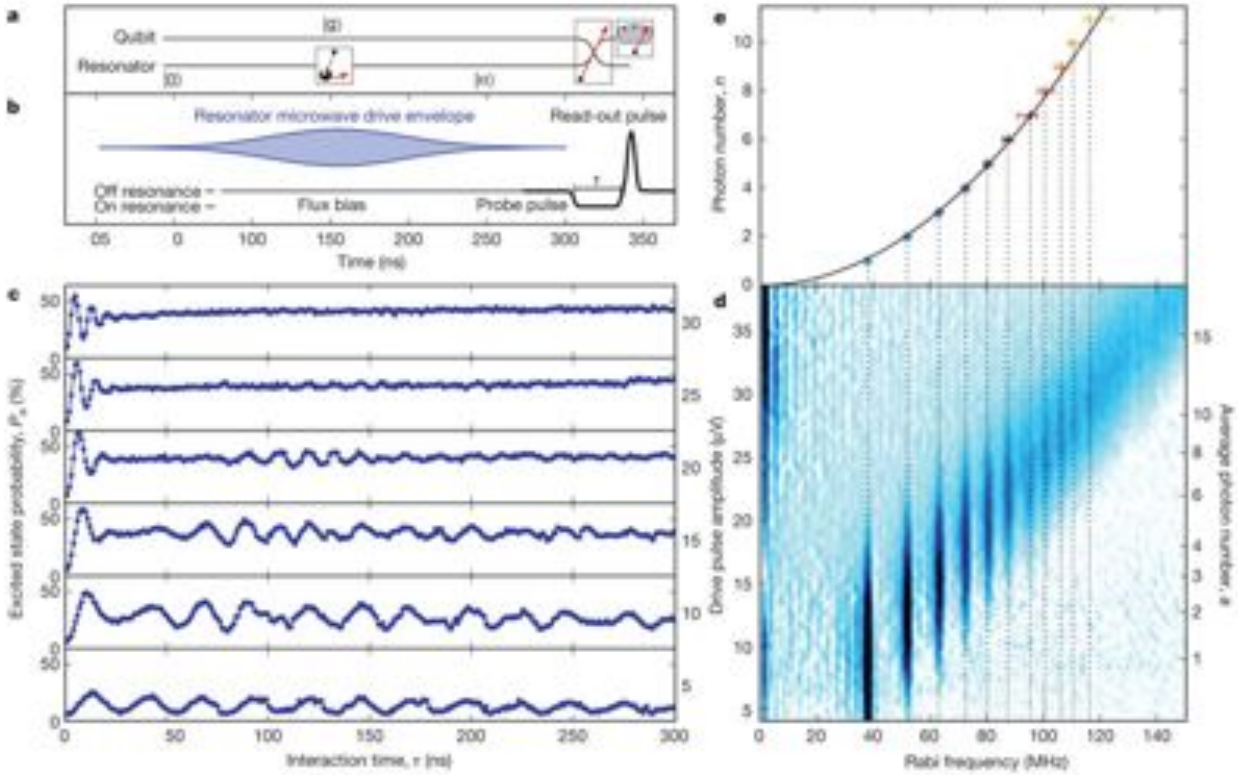

Fig.d at right shows (in color code) the amplitude of the Fourier components of the Rabi signal versus their frequency (horizontal axis) and versus the field amplitude α (vertical axis). Fig.e shows the frequencies of the various Fourier component as a function of their rank, i.e. the photon number. The experimental points fall as expected on a parabola.

Comparison with ion trap and Cavity QED experiments

The deterministic preparation of mechanical oscillator Fock states has been realized with trapped ions, according to the same method as the one described here in Circuit QED (experiments by the D.Wineland and R.Blatt groups in Boulder and Innsbruck). Rabi oscillations resulting from the coupling of a qubit to a harmonic oscillator in a coherent state have also been observed in 1996 on trapped ions and in cavity QED with Rydberg atoms. These experiments had already revealed the discrete naure of the harmonic oscillator energy scale by exhibiting discrete Fourier components in the Rabi oscillation signals. The figures below allow us to compare the results of these two experiments with the Circuit QED one.

Circuit QED:
M.Hofheinz et al, Nature ***454****, 310 (2008)*

The same coherent state « signature » in 3 experiments

Trapped ions:
Meekhof et al, PRL, 76, 1796 (1996).

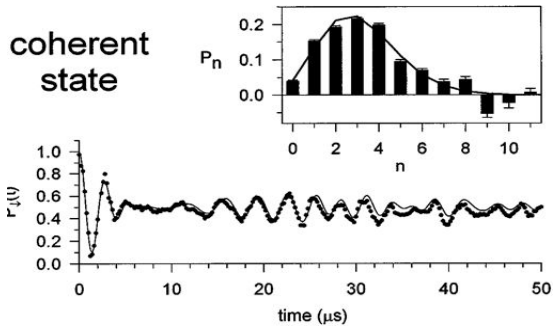

CQED:
Brune et al, PRL, 76, 1800 (1996)

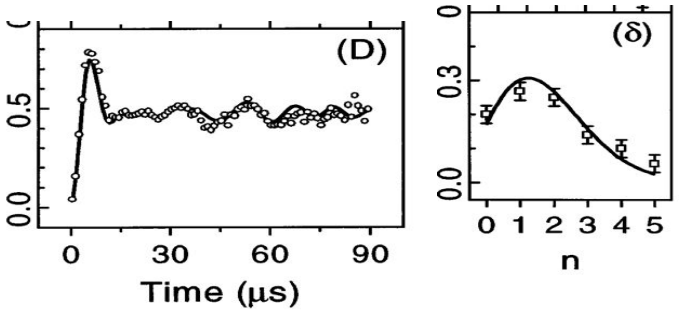

VI-B.

Synthesis of an arbitrary state of a radiofrequency resonator in Circuit QED

Arbitrary field state synthesis procedure in Circuit QED

The deterministic method to prepare Fock states of an rf resonator R makes use of a qubit Q coupled to R and combines two kinds of operations: Q rotations implying an energy exchange with a classical rf source and Rabi oscillations exchanging excitation between Q and R. By combining these operations with qubit phase shifts (amounting to Q-rotations around Oz), it is in fact possible to synthesize deterministically not only Fock states , but an arbitrary pure state $|\psi\rangle$ given by its expansion over the Fock state basis:

$$|\psi\rangle = \sum_n C_n |n\rangle \quad (6-1)$$

where the C_n 's are arbitrary complex amplitudes. Starting from state $|g,0\rangle$, a determined sequence of Q-rotations and Q-R Rabi oscillations leads to the final state $|g\rangle|\psi\rangle$, unenantengled tensor product of R in the desired state and Q in state $|g\rangle$. In order to program the sequence of operations, it is convenient to consider the reverse process: how to go from $|g\rangle|\psi\rangle$ to $|g\rangle|0\rangle$ by a sequence of such operations? Once this problem is solved, we only need to apply the inverse operations, in the reverse order, to go from $|g\rangle|0\rangle$ to $|g\rangle|\psi\rangle$. This systematic procedure has been proposed by Law and Eberly in 1996 (PRL **76**, 1055) and has been demonstrated in 2003 on a trapped ion (Ben Kish et al, PRL **90**, 037902), a system which obeys an evolution equation similar to that of CQED. The same procedure has been recently applied in Circuit QED by the J.Martinis group. We analyze here the principle of this method before describing this experiment.

Elementary operations for the arbitrary state synthesis of a field resonator

The Law and Eberly method applied to Circuit QED combines:

• Rotations by tunable angle ϕ of Q around the Ox axis of Bloch sphere, realized with rf pulses (Q and R being off-resonant):

$$R_x(\phi) = e^{-i\phi\sigma_x/2} = \cos\frac{\phi}{2} I - i\sin\frac{\phi}{2}\sigma_x \quad (6-2)$$

• Rotations of Q around Oz by angle χ, realized by producing a phase-shift between states e and g. The qubit, detuned by Δ from the resonator, is left to evolve freely during time t such that $\Delta t=\chi$. In this way, the following rotation is achieved (in the frame rotating at the frequency of the resonator):

$$R_z(\chi) = e^{-i\chi\sigma_z/2} \quad (6-3)$$

• Energy swaps by Rabi oscillation between Q and R, tuned in exact resonance. The evolution during time τ of the Q+R system, expressed in the basis of the combined states $|g,n+1\rangle$, $|e,n\rangle$ is described by the operator:

$$U_S = e^{-i\frac{\Omega\sqrt{n+1}\,\tau}{2}\sigma_x} = \cos\frac{\Omega\sqrt{n+1}\,\tau}{2} I - i\sin\frac{\Omega\sqrt{n+1}\,\tau}{2}\sigma_x \quad (6-4)$$

or, explicitely:

$$|g,n+1\rangle \xrightarrow{U_S} \cos\frac{\Omega\sqrt{n+1}\,\tau}{2}|g,n+1\rangle - i\sin\frac{\Omega\sqrt{n+1}\,\tau}{2}|e,n\rangle$$

$$|e,n\rangle \xrightarrow{U_S} -i\sin\frac{\Omega\sqrt{n+1}\,\tau}{2}|g,n+1\rangle + \cos\frac{\Omega\sqrt{n+1}\,\tau}{2}|e,n\rangle \quad (6-5)$$

Note the $\pi/2$ phase difference between the amplitudes of the two state components

State synthesis in Circuit QED: an example

Let us illustrate the method on a specific example. Suppose we want to prepare the state $|\psi\rangle = |1\rangle+i|3\rangle$ and let us start by determining the sequence of operations leading from $|g\rangle|\psi\rangle$ to $|g\rangle|0\rangle$. The idea is to suppress step by step the state component with the largest photon number, so as to come back progressively to state $|0\rangle$. We thus start by applying a Q-R Rabi oscillation of duration $\tau_3=\pi/\Omega\sqrt{3}$ adjusted to realize the transformation:

$$|g,3\rangle \xrightarrow[\tau_3=\pi/\Omega\sqrt{3}]{} -i|e,2\rangle \quad (6-6)$$

Starting from state $|g,\psi\rangle$, this transformation yields (see equ. 6-5):

$$\frac{1}{\sqrt{2}}\left[|g,1\rangle+i|g,3\rangle\right] \xrightarrow[\tau_3]{} |\Psi_1\rangle = \frac{1}{\sqrt{2}}\cos\frac{\Omega\tau_3}{2}|g,1\rangle - \frac{i}{\sqrt{2}}\sin\frac{\Omega\tau_3}{2}|e,0\rangle + \frac{1}{\sqrt{2}}|e,2\rangle = \frac{1}{\sqrt{2}}\cos\left(\frac{\pi}{2\sqrt{3}}\right)|g,1\rangle - \frac{i}{\sqrt{2}}\sin\left(\frac{\pi}{2\sqrt{3}}\right)|e,0\rangle + \frac{1}{\sqrt{2}}|e,2\rangle \quad (6-7)$$

As planned, the 3 photon component has disappeared. We then apply on Q the rotation $\exp[-i\pi\sigma_x/2]=-i\sigma_x$ which exchanges $|e\rangle$ and $|g\rangle$ and leads to the Q-R combined state:

$$|\Psi_2\rangle = -\frac{1}{\sqrt{2}}\sin\left(\frac{\pi}{2\sqrt{3}}\right)|g,0\rangle - \frac{i}{\sqrt{2}}\left[|g,2\rangle+\cos\left(\frac{\pi}{2\sqrt{3}}\right)|e,1\rangle\right] \quad (6-8)$$

The next step must suppress the 2 photon component by transforming the $|g,2\rangle$, $|e,1\rangle$ superposition in equ.(6-8) into $|e,1\rangle$ by a Rabi swap. To achieve this, we must first adjust the phases and introduce a $\pi/2$ phase-shift between the states $|e\rangle$ and $|g\rangle$. This is realized by a Q rotation around Oz by the angle $3\pi/2$, $R_z=\exp[-3i\pi\sigma_z/4]$, which leads to the state:

$$|\Psi_3\rangle = \frac{e^{-i\pi/4}}{\sqrt{2}}\sin\left(\frac{\pi}{2\sqrt{3}}\right)|g,0\rangle + \frac{e^{i\pi/4}}{\sqrt{2}}\left[|g,2\rangle+i\cos\left(\frac{\pi}{2\sqrt{3}}\right)|e,1\rangle\right] \quad (6-9)$$

By applying next a Rabi oscillation of convenient duration we transform the bracketed term in equ.(6-9) into the state $|e,1\rangle$ (see next page).

State synthesis: a simple example (cont'd)

The Q-R Rabi swap which suppresses the 2 photon component in (6-9) has an angle different from that of the swap which cancelled the n=3 state. A π-swap lasting a time $\pi/\Omega\sqrt{2}$ transforms $|g,2\rangle$ in (6-9) into $|e,1\rangle$, but introduces a new $|g,2\rangle$ component due to the evolution of the $|e,1\rangle$ part in (6-9). We must apply U_S for a time different from $\pi/\Omega\sqrt{2}$. To find out this time, we express the bracketed term in (6-9) as:

$$|g,2\rangle + i\cos\left(\frac{\pi}{2\sqrt{3}}\right)|e,1\rangle = \sqrt{1+\cos^2\left(\frac{\pi}{2\sqrt{3}}\right)}\left[\cos\frac{\Theta}{2}|g,2\rangle - i\sin\frac{\Theta}{2}|e,1\rangle\right] \quad (6-10)$$

the angle Θ being defined by the relations:

$$\cos\frac{\Theta}{2} = 1/\sqrt{1+\cos^2\frac{\pi}{2\sqrt{3}}} \quad ; \quad \sin\frac{\Theta}{2} = -\cos\frac{\pi}{2\sqrt{3}}/\sqrt{1+\cos^2\frac{\pi}{2\sqrt{3}}} \quad (6-11)$$

We then deduce from (6-5) that the evolution of $|\Psi_3\rangle$ during time τ leads to:

$$|\Psi_4\rangle = \frac{e^{-i\pi/4}}{\sqrt{2}}\sin\left(\frac{\pi}{2\sqrt{3}}\right)|g,0\rangle + \frac{e^{i\pi/4}}{\sqrt{2}}\sqrt{1+\cos^2\frac{\pi}{2\sqrt{3}}}\left[\cos\left(\frac{\Theta+\Omega\sqrt{2}\tau}{2}\right)|g,2\rangle - i\sin\left(\frac{\Theta+\Omega\sqrt{2}\tau}{2}\right)|e,1\rangle\right] \quad (6-12)$$

Hence for $\tau = \dfrac{\pi-\Theta}{\Omega\sqrt{2}}$: $|\Psi_4\rangle = \dfrac{e^{-i\pi/4}}{\sqrt{2}}\sin\left(\dfrac{\pi}{2\sqrt{3}}\right)|g,0\rangle - i\dfrac{e^{i\pi/4}}{\sqrt{2}}\sqrt{1+\cos^2\dfrac{\pi}{2\sqrt{3}}}\,|e,1\rangle$ (6-13)

After a Q-rotation by angle π, $|\Psi_4\rangle$ becomes:

$$|\Psi_5\rangle = -i\frac{e^{-i\pi/4}}{\sqrt{2}}\left[\sin\left(\frac{\pi}{2\sqrt{3}}\right)|e,0\rangle + \sqrt{1+\cos^2\frac{\pi}{2\sqrt{3}}}\,|g,1\rangle\right] \quad (6-14)$$

An R_Z rotation introducing a $\pi/2$ phase-shift between the $|\Psi_5\rangle$ components leads to $|\Psi_6\rangle$, a superposition of $|e,0\rangle$ and $|g,1\rangle$ which a Rabi swap of adjusted angle changes into $|\Psi_7\rangle=|e,0\rangle$. A final rf pulse transforms it into $|\Psi_8\rangle=|g,0\rangle$. Eight operations are thus required to go from $|g,\Psi\rangle$ to $|g,0\rangle$. By applying in reverse order the 8 inverse operations, we synthesise from $|g,0\rangle$ the desired state $|g\rangle[|1\rangle+i|3\rangle]$.

Arbitrary state synthesis: another example

In our first example, all the Q rotations had an angle $\phi = \pi$. In general, this angle must also be adjusted in a more subtle way. Suppose for instance that we want to generate the state:

$$|\psi\rangle = |0\rangle + |1\rangle + |2\rangle \quad (6-15)$$

We start as before by a Rabi swap with an angle π coupling $|g,2\rangle$ and $|e,1\rangle$:

$$|g,\psi\rangle = |g,0\rangle + |g,1\rangle + |g,2\rangle \longrightarrow |\Psi_1\rangle = |g,0\rangle + \left[\cos\frac{\pi}{2\sqrt{2}}|g,1\rangle - i\sin\frac{\pi}{2\sqrt{2}}|e,0\rangle\right] - i|e,1\rangle \quad (6-16)$$

The n=2 component is cancelled. In order to then suppress the n=1 component, we must manage so that $|\Psi\rangle$ has only a $|g,1\rangle$ term, without $|e,1\rangle$ contribution, since this last term would, under Rabi oscillation, make a $|g,2\rangle$ term reappear. The one photon part in (6-16) corresponds to the Q state:

$$|\psi_{Q1}\rangle = \cos\frac{\pi}{2\sqrt{2}}|g\rangle - i|e\rangle = \sqrt{1+\cos^2\frac{\pi}{2\sqrt{2}}}\left[\cos\frac{\theta}{2}|g\rangle - i\sin\frac{\theta}{2}|e\rangle\right];$$

$$with \quad \cos\frac{\theta}{2} = \cos\frac{\pi}{2\sqrt{2}} \Big/ \sqrt{1+\cos^2\frac{\pi}{2\sqrt{2}}} \quad ; \quad \sin\frac{\theta}{2} = 1 \Big/ \sqrt{1+\cos^2\frac{\pi}{2\sqrt{2}}} \quad (6-17)$$

The Q rotation which brings this state into $|g\rangle$ is not a rotation of angle $\phi=\pi$, as was the case in the first example, but rather a rotation of angle $\phi=-\theta$ around Ox:

$$R_x(-\theta)|\psi_{Q1}\rangle = \sqrt{1+\cos^2\frac{\pi}{2\sqrt{2}}}\left[\cos\frac{\theta}{2}I + i\sin\frac{\theta}{2}\sigma_x\right]\left[\cos\frac{\theta}{2}|g\rangle - i\sin\frac{\theta}{2}|e\rangle\right] = \sqrt{1+\cos^2\frac{\pi}{2\sqrt{2}}}|g\rangle \quad (6-18)$$

The $|\Psi_1\rangle$ state then becomes a superposition of $|g,0\rangle$, $|e,0\rangle$ and $|g,1\rangle$. A phase shift combined to a Rabi oscillation of adjusted angle then transforms it into a superposition of $|g,0\rangle$ and $|e,0\rangle$. A last Q rotation then brings the system into $|g,0\rangle$.

Sketch schematizing the state synthesis

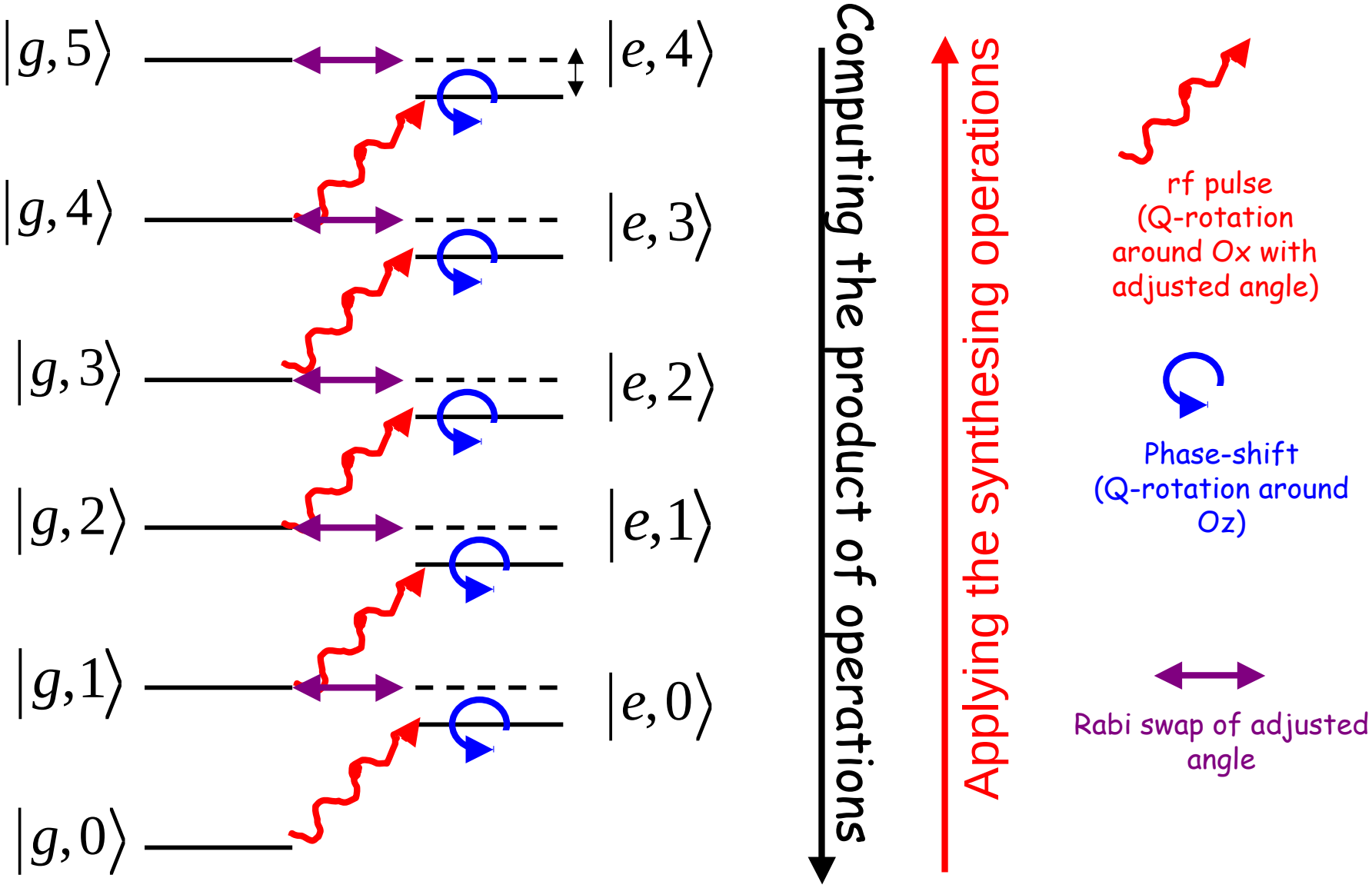

Arbitrary state synthesis in Circuit QED: the experiment

*M Hofheinz et al. Nature **459**, 546-549 (2009)*

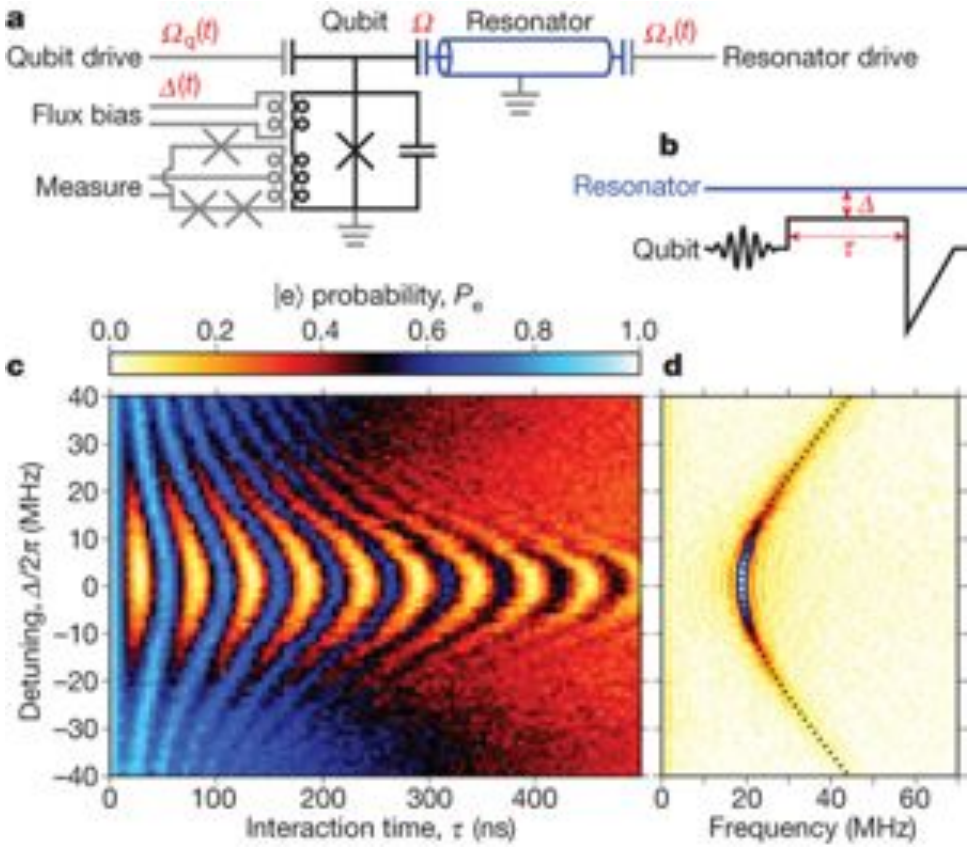

Fig a: Scheme of circuit (description of components in lecture 5).

b: Sequence of operations realizing the $|e,0\rangle \rightarrow |g,1\rangle$ Rabi swap. Q in $|g\rangle$, largely detuned from R initially in vacuum ($|0\rangle$), undergoes a π rf pulse (wavy line) bringing it in $|e\rangle$. Q is then tuned closer to resonance (detuning Δ) and the Q-R system evolves during time τ. Q is finally measured after a large flux bias pulse has brought level e close to the effective potential barrier maximum. By averaging over a large set of realizations, P_e is reconstructed.

We observe a Rabi oscillation with minimal frequency $\Omega/2\pi$= 19 MHz for Δ=0. We see that the oscillation frequency increases and that its amplitude decreases when $|\Delta|$ increases from 0.

d: Fourier transform of signal shown in Figc, showing the hyperbolic variation as $[\Delta^2+\Omega^2]^{1/2}$ of the Rabi frequency versus Δ.

Arbitrary state synthesis (cont'd)

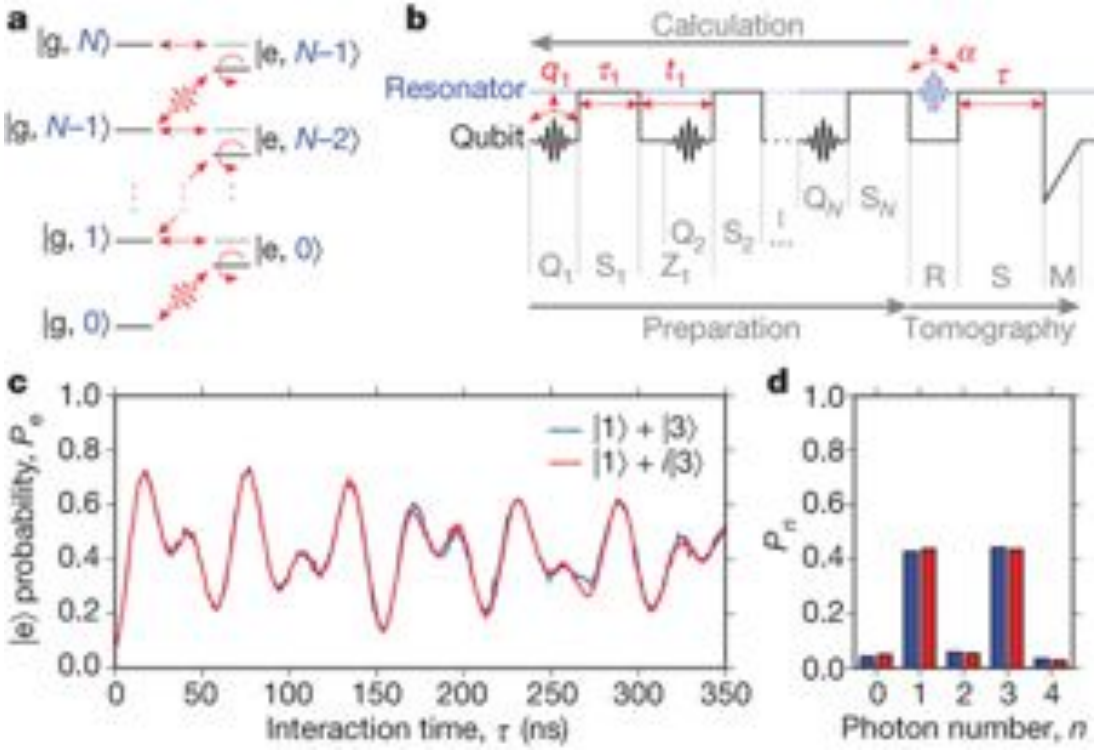

a: diagram showing the sequence of operations on the energy ladder of the Q-R system (see 2 pages above).

b: sequence of operations for preparing and measuring the state of R. The rf pulses noted q_i (wavy lines) are applied when Q and R are largely off-resonant. The Rabi oscillations which swap a quantum between Q and R are called S_i. They are achieved by tuning Q and R ar resonance (Δ=0). The phase-shifts (rotations around Oz) noted Z_i are realized by letting Q evolve out of resonance with R during an adjusted time interval. The 8 operations shown here prepare $|1\rangle+i|3\rangle$. (see above).

Once the state has been generated, a tomographic sequence is realized in order to reconstruct it. R, being largely detuned from Q, is fed by a coherent field of amplitude $-\alpha$. Q and R are then tuned into resonance and the Rabi oscillation is realized during a time τ. The state of Q is finally detected and the probability $P_e(\tau)$ is obtained from a large set of runs. We recall below how this sequence of operations makes it possible to reconstruct fully the state of R (see also lecture 3 for a similar reconstruction scheme in cavity QED).

c: When no field is injected in R during the tomographic process (α=0), $P_e(\tau)$ simply yields the Rabi signal in the synthesized field. The figure shows this signal versus time following the preparation of the states $|1\rangle+|3\rangle$ (blue line) and $|1\rangle+i|3\rangle$ (red line). The beating between the frequencies Ω and $\Omega\sqrt{3}$ is conspicuous.

d: The Fourier transform of the Rabi signal yields the photon number probability distributions in these wo states (in blue and red). This distribution does not provide any information about the phases of the probability amplitudes and does not allow us to distinguish these two states.

A reminder about state reconstruction by direct determination of the Wigner function

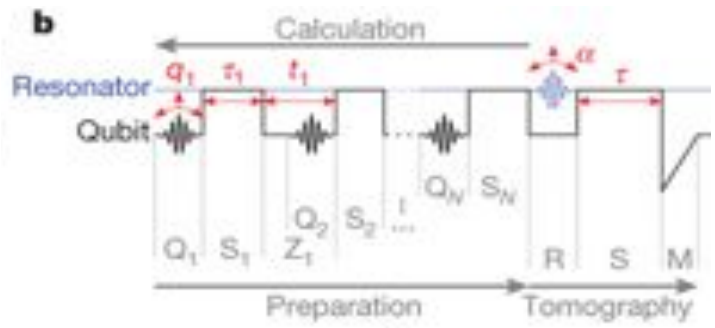

We have recalled in Lecture 3 how to reconstruct the Wigner function of an oscillator at point α in phase space by performing photon number distribution measurements on the oscillator state displaced by $-\alpha$. The procedure is based on the formula linking $W(\alpha)$ to the expectation value of the photon parity operator $\mathcal{P}$ in the displaced state:

$$W(\alpha)=\frac{2}{\pi}Tr\left[D(-\alpha)\rho D(\alpha)\mathcal{P}\right]=\frac{2}{\pi}\sum_n(-1)^n\Pi^{(\alpha)}(n)\quad(\Pi^{(\alpha)}(n):\textit{probability of } n \textit{ photons in displaced state})\quad(6-19)$$

This method is applied in the Circuit QED experiment. The desired state is synthesized by the procedure analyzed above. Then a coherent field with amplitude $-\alpha$ is injected in R to displace this state in phase space. R is then tuned into resonance with Q during a variable time τ and, by repeating the sequence many times, the Rabi oscillation in the displaced field is obtained. A Fourier transform yields the weights of the frequency components in this signal, which give the probabilities $\Pi^{(\alpha)}(n)$ for finding n photons un the state displaced by $-\alpha$. Formula (6-19) finally yields $W(\alpha)$ for this value of α. By varying α, the W function is reconstructed. The density operator ρ in the basis of the quadrature eigenstates is then given by:

$$\langle x+u/2|\rho|x-u/2\rangle=\int dp\, e^{2ipu}W(x,p)\quad;\quad\alpha=x+ip\quad(6-20)$$

($|x \pm u/2\rangle$ is the eigenstate with eigenvalue $x\pm u/2$ of the quadrature operator $(a+a^{\dagger})/2$). From this expression, ρ in the Fock state basis is derived by a mere basis change.

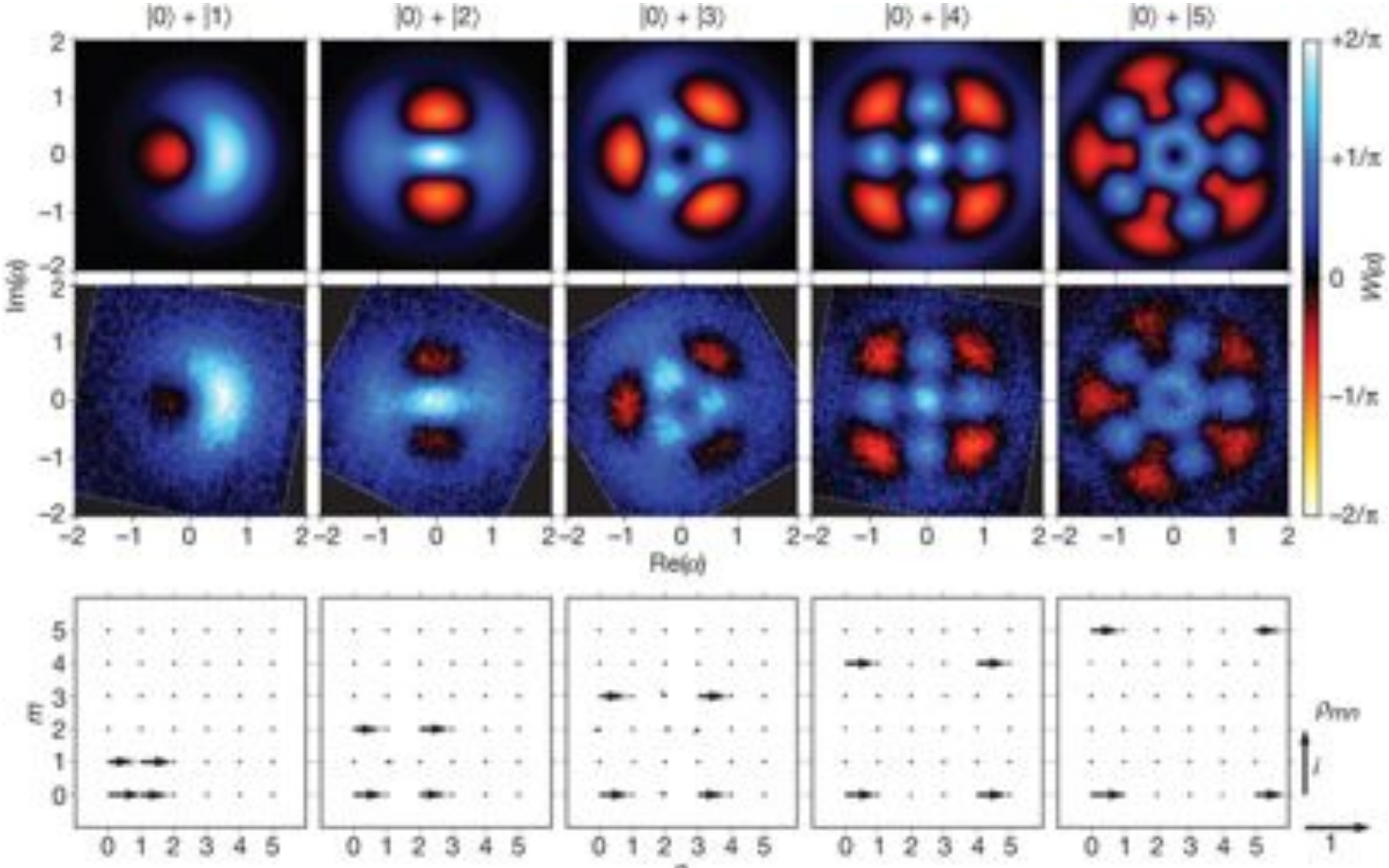

Synthesis and reconstruction of the states $|0\rangle+|n\rangle$ with n=1,2,3,4 et 5. The theoretical (upper line) and experimental (lower line) Wigner functions $W(\alpha)$ are compared. The red zones correspond to negative W values. The third line of frames shows the corresponding density matrices in Fock state basis (horizontal arrows: real numbers, vertical arrows: imaginary numbers). Experimental values are in black, theoretical ones in grey.

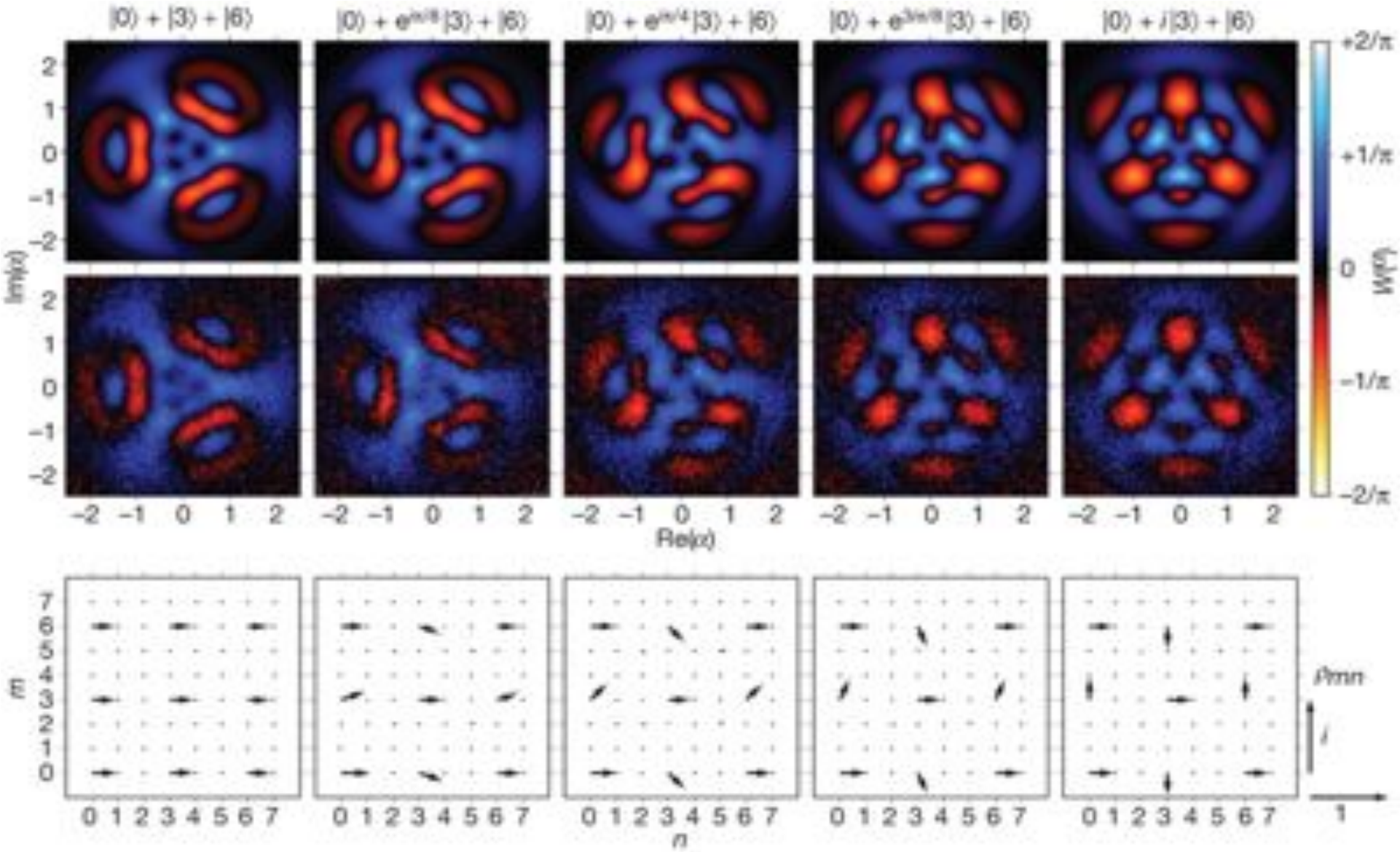

Synthesis and reconstruction of states |0>+exp(ikπ/8)|3>+|6> with k=0,1,2,3,4. The theoretical Wigner functions (first line) are compared with the measured ones (second line). The third line shows the corresponding density matrices. Same conventions as in previous page.

Comparison with CQED

Circuit QED and Cavity QED allow us to prepare and reconstruct non-classical field states with similar methods. In both cases, states can also be reconstructed versus time, yielding decoherence movies. Data collection is faster in Circuit QED.

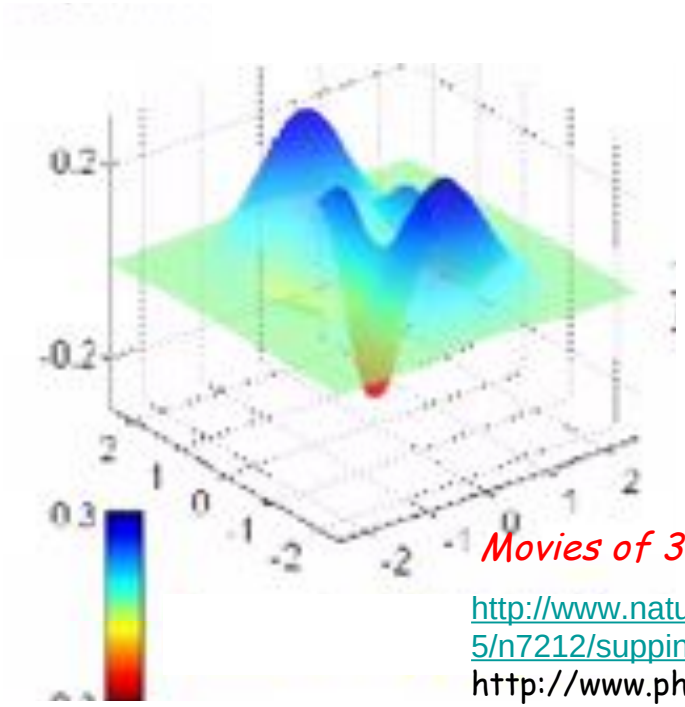

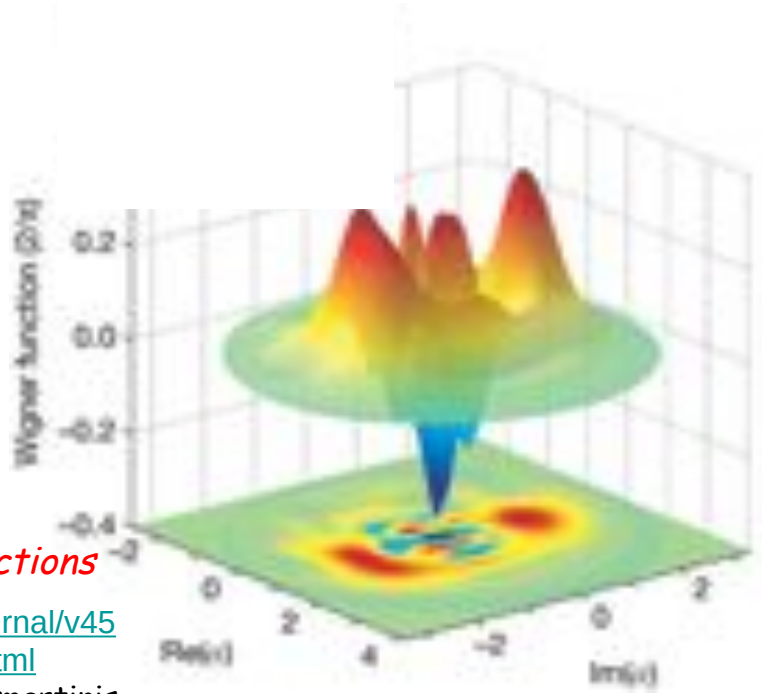

Movies of 3D Wigner functions

http://www.nature.com/nature/journal/v455/n7212/suppinfo/nature07288.html

http://www.physics.ucsb.edu/~martinisgroup/movies/Movie_odd.avi

$$\left|\alpha e^{i\chi}\right\rangle - \left|\alpha e^{-i\chi}\right\rangle \quad (\alpha = \sqrt{2} \quad ; \quad \chi = 0,5\pi)$$

« cat » state prepared and reconstructed in Circuit QED (Martinis group, USBC)

$$\left|\alpha e^{i\chi}\right\rangle + \left|\alpha e^{-i\chi}\right\rangle \quad (\alpha = \sqrt{3,5} \quad ; \quad \chi = 0,37\pi)$$

« cat » state prepared and reconstructed in CQED at ENS (see lecture 3)

VI-C

Synthesis of non-local entangled field states (NOON states of two resonators)

*H.Wang et al, Phys.Rev.Lett. **106**, 060401 (2011)*

Synthesis of NOON states in Circuit QED

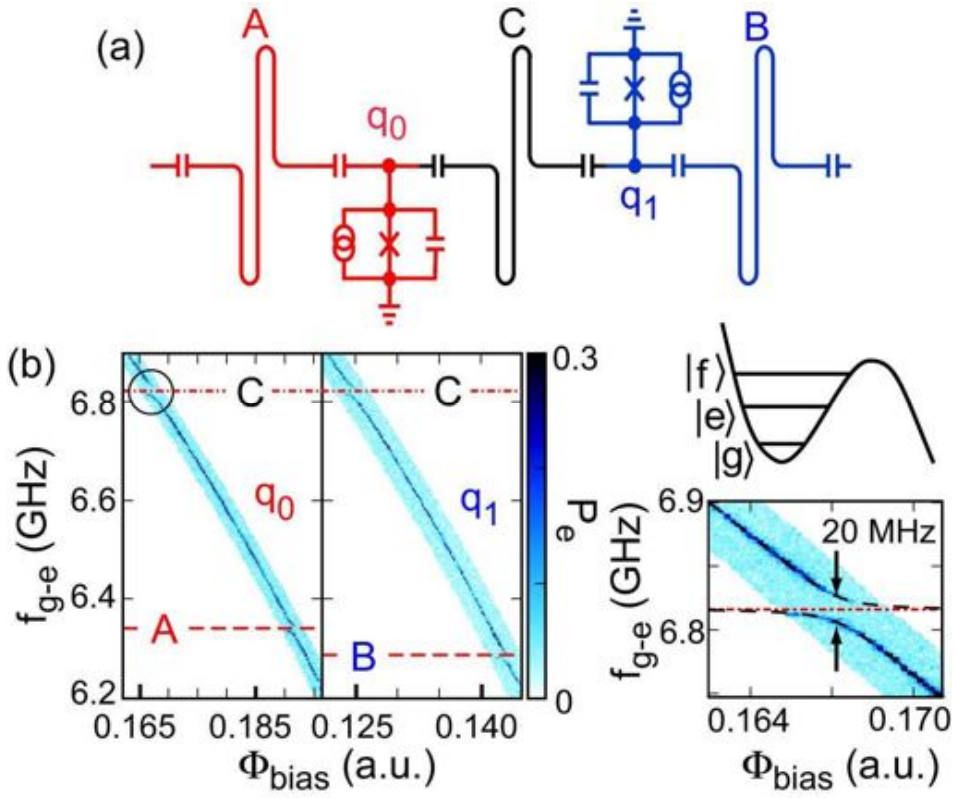

The goal of the experiment is to prepare *NOON states* of two resonators A and B:

$$|\Psi\rangle_{AB} = \frac{1}{\sqrt{2}}\left(|N\rangle_A|0\rangle_B + |0\rangle_A|N\rangle_B\right) \quad (6-21)$$

The circuit involves three resonators A,B and C and two phase qubits q_0 and q_1 respectively coupled to A and C (qubit q_0) and B and C (qubit q_1). Each qubit has three levels relevant to the experiment: the two logical qubit states, g and e, and a third level, f, linked to e by a transition whose frequency is different from that of the e→g transition: the qubits are in fact qutrits. The resonator frequencies are all different, allowing the qubits to be coupled selectively with each resonator.

In a preliminary calibration experiment, the qubit spectroscopy is realized by recording their frequencies f_{ge} and f_{ef} versus the flux biases (Φ_{bias}). Curves with anticrossings centered at the frequencies of the A and C resonators for qubit q_0, at the frequencies of qubits B and C for qubit q_1 are obtained. Pointing these frequencies allow the experimenters to calibrate the flux biases required to tune into resonance the qubits with their respective resonators on the g→e and e→f transitions.

Preparing state |1,0>+|0,1>

Entangling the two qubits via their coupling to C: q_0, q_1 and C are initialized in their ground states, a π pulse is then applied on q_0 (qubit rotation around 0x), followed by a $\pi/2$ Rabi swap between q_0 and C and a 3π Rabi swap between C and q_1. These operations are achieved by successive tuning q_0, q_1 in and out of resonance with C:

$$|g,g\rangle_{q_0q_1}\otimes|0\rangle_C \xrightarrow{\text{pulse } \pi\ q_0} -i|e,g\rangle_{q_0q_1}|0\rangle_C \xrightarrow{\text{pulse Rabi } \pi/2\ q_0-C} \frac{1}{\sqrt{2}}\left[|e,g\rangle_{q_0q_1}|0\rangle_C - i|g,g\rangle_{q_0q_1}|1\rangle_C\right]$$

$$\xrightarrow{\text{pulse Rabi } 3\pi\ q_1-C} \frac{1}{\sqrt{2}}\left(|e,g\rangle_{q_0q_1}+|g,e\rangle_{q_0q_1}\right)|0\rangle_C \quad (6-22)$$

The two qubits are thus entangled via their successive couplings to C which acts as an entanglement catalyst and ends up non-entangled with the qubits, in its initial state. This operation is anologous to the entanglement procedure used in CQED to entangle two Rydberg atoms crossing succesively the cavity.

Transfering excitation and entanglement to A and B: q_0 and q_1 are resonantly coupled one after the other with A and B, initially both in state |0>, realizing energy swaps between the qubits and the resonators (π Rabi pulses q_0-A and q_1-B):

$$\frac{1}{\sqrt{2}}\left(|e,g\rangle_{q_0q_1}+|g,e\rangle_{q_0q_1}\right)|0\rangle_A|0\rangle_B \xrightarrow{\text{pulse Rabi } \pi\ q_0-A} \frac{1}{\sqrt{2}}\left[-i|g,g\rangle_{q_0q_1}|1\rangle_A|0\rangle_B + |g,e\rangle_{q_0q_1}|0\rangle_A|0\rangle_B\right]$$

$$\xrightarrow{\text{pulse Rabi } \pi\ q_1-B} \frac{-i}{\sqrt{2}}\left(|1\rangle_A|0\rangle_B+|0\rangle_A|1\rangle_B\right)|g,g\rangle_{q_0q_1} \quad (6-23)$$

The entangled state |1,0>+|0,1> is thus prepared. It corresponds to a photon being delocalized between the two resonators. The qubits end up non-entangled with the fields and are back to their initial state. Similar procedures have been applied in ion trap and CQED physics.

Preparing NOON states with N>1

Transfering entanglement from |e,g>+|g,e> to |f,g>+|g,f> by single qubit operations:

$$|e,g\rangle+|g,e\rangle \xrightarrow[\pi \text{ pulses on } e\to f \text{ transition for } q_0 \text{ and } q_1]{} |f,g\rangle+|g,f\rangle \quad (6-24)$$

Coupling q_0 to A and q_1 to B, resonant on the f→e transition to exchange the qubit excitation with the resonators (swapping):

$$\left(|f,g\rangle+|g,f\rangle\right)|0_A,0_B\rangle \xrightarrow[\text{pulses Rabi } \pi \text{ transition } e\to f]{} |e,g\rangle|1_A,0_B\rangle+|g,e\rangle|0_A,1_B\rangle \quad (6-25)$$

Contrary to previous case, the two resonator fields and the qubits remain entangled. It is then possible to pursue the procedure by re-exciting the qubits from e to f:

$$|e,g\rangle|1_A,0_B\rangle+|g,e\rangle|0_A,1_B\rangle \xrightarrow[\text{pulses } \pi \text{ sur transition } e\to f]{} |f,g\rangle|1_A,0_B\rangle+|g,f\rangle|0_A,1_B\rangle \quad (6-26)$$

The f→ e excitation is again transfered to A and B (this swapping takes a time √2 smaller than at previous step):

$$|f,g\rangle|1_A,0_B\rangle+|g,f\rangle|0_A,1_B\rangle \xrightarrow[\text{pulses Rabi } \pi \text{ transition } e\to f]{} |e,g\rangle|2_A,0_B\rangle+|g,e\rangle|0_A,2_B\rangle \quad (6-27)$$

To prepare more excited NOON states, the process is iterated: :

$$|e,g\rangle|2_A,0_B\rangle+|g,e\rangle|0_A,2_B\rangle \xrightarrow[\text{pulses } \pi\ e\to f]{} \xrightarrow[\text{pulses Rabi } \pi]{} \cdots\cdots \to |e,g\rangle|(N-1)_A,0_B\rangle+|g,e\rangle|0_A,(N-1)_B\rangle \quad (6-28)$$

At the last step, the qubits are tuned into resonance with A and B respectively, this time on the e→ g (not e→ f) transition, realizing a last Rabi swap:

$$|e,g\rangle|(N-1)_A,0_B\rangle+|g,e\rangle|0_A,(N-1)_B\rangle \xrightarrow[\text{pulses } \pi \text{ Rabi transition } e\to g]{} |g,g\rangle\left(|N_A,0_B\rangle+|0_A,N_B\rangle\right) \quad (6-29)$$

A NOON state is generated, un-entangled with the qubits back in ground state.

Photon number probability distribution in NOON states

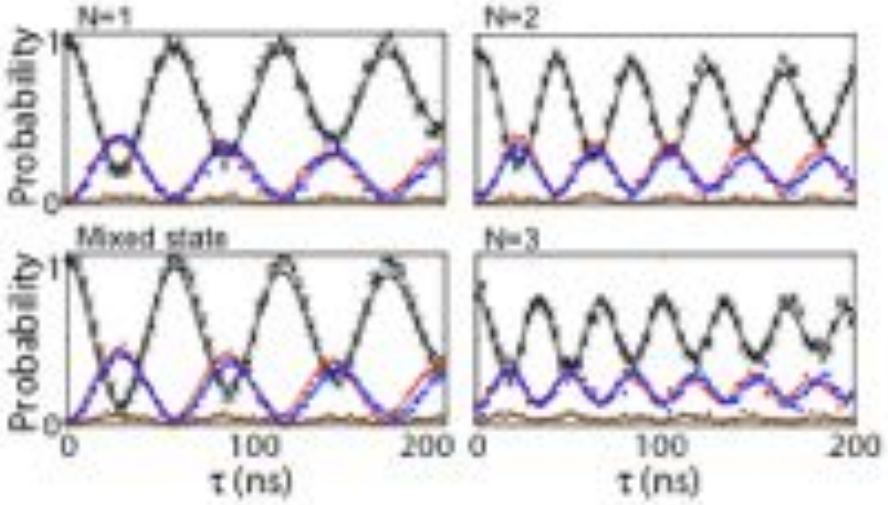

$$P_{e,e}(\tau) = \sum_{n_A,n_B} \Pi(n_A,n_B) \sin^2 \frac{\Omega\sqrt{n_A}\tau}{2} \sin^2 \frac{\Omega\sqrt{n_B}\tau}{2}$$

$$P_{e,g}(\tau) = \sum_{n_A,n_B} \Pi(n_A,n_B) \sin^2 \frac{\Omega\sqrt{n_A}\tau}{2} \cos^2 \frac{\Omega\sqrt{n_B}\tau}{2}$$

$$P_{g,e}(\tau) = \sum_{n_A,n_B} \Pi(n_A,n_B) \cos^2 \frac{\Omega\sqrt{n_A}\tau}{2} \sin^2 \frac{\Omega\sqrt{n_B}\tau}{2}$$

$$P_{g,g}(\tau) = 1 - P_{e,g}(\tau) - P_{g,e}(\tau) - P_{e,g}(\tau)$$

After state preparation, q_0 is coupled to A and q_1 to B (A and B tuned into resonance during time τ on the g →e transition) before detecting the qubits. By repeating the procedure, the coincidence probabilities $P_{e,e}(\tau)$, $P_{e,g}(\tau)$, $P_{g,e}(\tau)$ and $P_{g,g}(\tau)$ are reconstructed. The figures at right show the results for the NOON states (N=1,2 and 3) and for a statistical mixture realized by preparing alternatively |1,0> and |0,1>. The P_{eg} and P_{ge} curves are in red and blue, P_{gg} in black and P_{ee}~ 0 in brown. For the most general double distribution of photons $\Pi(n_A,n_B)$, the expected probabilities are given at right. For |N,0>+|0,N> the double probability is:

$$\Pi(n_A,n_B) = \frac{1}{2}\left(\delta_{n_A,N}\delta_{n_B,0} + \delta_{n_A,0}\delta_{n_B,N}\right) \quad (5-31)$$

and, from (5-30) we get:

$$P_{e,e}(\tau) = 0 \quad ; \quad P_{e,g}(\tau) = P_{g,e}(\tau) = \frac{1}{2}\sin^2\left(\frac{\Omega\sqrt{N}\tau}{2}\right)$$

$$P_{g,g}(\tau) = \cos^2\left(\frac{\Omega\sqrt{N}\tau}{2}\right) \quad (5-32)$$

There is good agreement between theory and experiment, but this test does not distinguish |1,0>+|0,1> from a mixture of |1,0> and |0,1> (compare the N=1 curve with that of mixed state).

Complete tomography of NOON states

The full reconstruction of the field state of the two resonators, *including information about the field coherences*, is achieved by generalizing the methods described in Lecture 3 in the case of a single cavity field in a CQED experiment. A double phase space displacement is achieved on the two field oscillators:

$$\rho_{AB} \xrightarrow[Displacement]{} \rho_{AB}^{(\alpha,\beta)} = D_A(-\alpha)D_B(-\beta)\rho_{AB}D_A(\alpha)D_B(\beta) \quad (5-33)$$

The double distribution of the photon number probability in the displaced state is:

$$\Pi^{(\alpha,\beta)}(n_A,n_B) = \langle n_A,n_B|\rho_{AB}^{(\alpha,\beta)}|n_A,n_B\rangle$$

$$= \sum_{\substack{m_A,m_B \\ p_A,p_B}} \langle n_A,n_B|D_A(-\alpha)D_B(-\beta)|m_A,m_B\rangle\langle m_A,m_B|\rho_{AB}|p_A,p_B\rangle\langle p_A,p_B|D_A(\alpha)D_B(\beta)|n_A,n_B\rangle \quad (5-34)$$

By choosing a set of displacements (α_k,β_l) corresponding to an ensemble of points in the double phase space, an ensemble of linear equations are obtained which express the $\Pi^{(\alpha,\beta)}(n_A,n_B)$ as combinations of the $\langle m_A,m_B|\rho|p_A,p_B\rangle$ elements of the density operator to be reconstucted. By solving these equations, one obtains in principle a set of equations expressing these elements as linear combinations of the $\Pi^{(\alpha,\beta)}(n_A,n_B)$:

$$\langle m_A,m_B|\rho_{AB}|p_A,p_B\rangle = \sum_{\substack{n_A,n_B \\ \alpha_k,\beta_l}} C_{\substack{n_A,n_B \\ \alpha_k,\beta_l}}^{(m_A,m_B \\ p_A,p_B)} \Pi^{(\alpha_k,\beta_l)}(n_A,n_B) \quad (5-35)$$

The $\Pi^{(\alpha,\beta)}(n_A,n_B)$ distributions are experimentally determined by recording the Rabi oscillations of the correlated qubit detection probabilities:

$$P_{e,g}^{(\alpha,\beta)}(\tau) = \sum_{n_A,n_B} \Pi^{(\alpha,\beta)}(n_A,n_B)\sin^2\frac{\Omega\sqrt{n_A}\tau}{2}\cos^2\frac{\Omega\sqrt{n_A}\tau}{2}; P_{g,e}^{(\alpha,\beta)}(\tau) = \sum_{n_A,n_B} \Pi^{(\alpha,\beta)}(n_A,n_B)\cos^2\frac{\Omega\sqrt{n_A}\tau}{2}\sin^2\frac{\Omega\sqrt{n_A}\tau}{2} \quad (5-36)$$

Complete tomography of NOON states (cont'd)

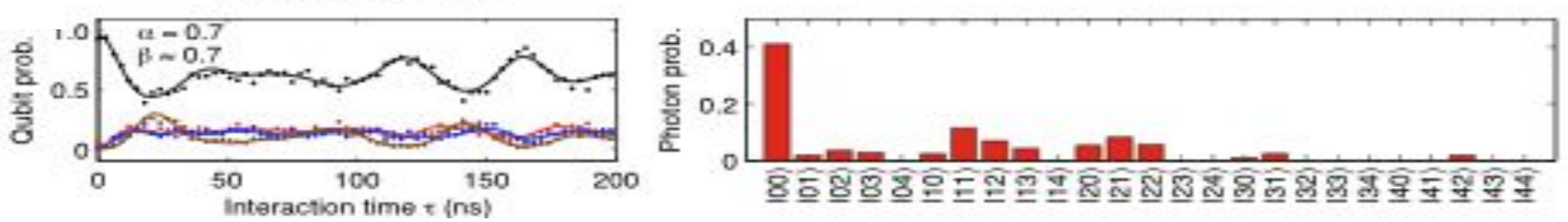

Reconstructing (at right) $\Pi^{(\alpha,\beta)}(n_A,n_B)$ for N=1 and $\alpha=\beta=0,7$ from the Rabi signals (at left) exhibiting $P_{e,g}(\tau)$ (red line), $P_{ge}(\tau)$ (blue line) and $P_{gg}(\tau) = 1-P_{eg}(\tau)-P_{ge}(\tau)$ (black line). The reconstruction is perfomed by a «best fit» of formulae (5-36), corrected by taking into account the known imperfections of the apparatus (for a similar discussion in the context of CQED, see lecture 3).

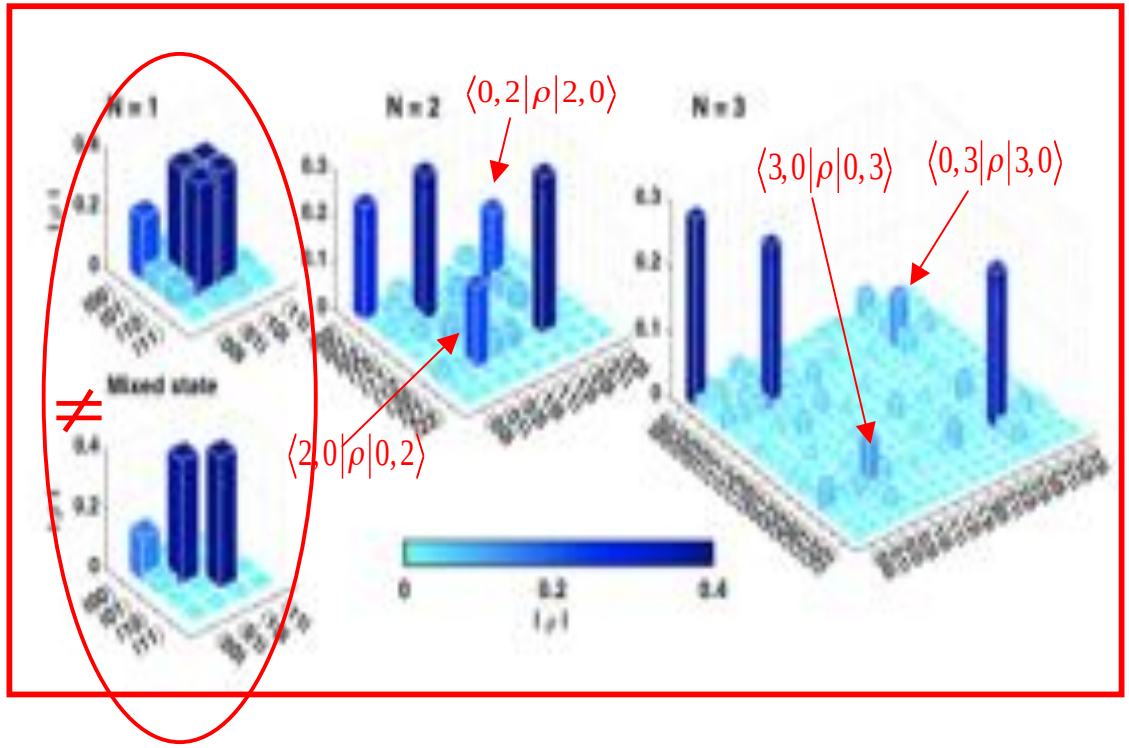

Knowing the $\Pi^{(\alpha,\beta)}(n_A,n_B)$, the matrix elements of the NOON states are obtained by an estimation method amounting to the inversion procedure described above. The figure at left shows the reconstructed ρ for N=1, 2 and 3 and for the mixed state [|1,0><1,0| + |0,1><0,1|]. The decay of the <N,0|ρ|0,N> elements is due to decoherence during the measuring sequences. The <0,0|ρ|0,0> peak, increasing with N, is due to imperfect qubits initial preparations.

Conclusion of sixth lecture

The experiments described in this lecture demonstrate the flexibility and the versatility of Circuit QED for the synthesis and reconstruction of non-classical field states stored in one or two rf resonators. The « size » of the accessible fields is limited by decoherence. In short, the number of operations required to synthesize a state with up to N photons is ~ kN with k~ 3 to 5. The time of an elementary operation is T_{op}~ 20 ns and each preparation sequence thus takes a time ~ kNT_{op} which must be smaller than the decoherence time T_c/N with T_c~1µs. Decoherence thus becomes significant when N ~ $(T_c/kT_{op})^{1/2}$ ~ 3. This order of magnitude is indeed the one indicated by the results of the previous page. Increasing the decoherence times should make it possible to extend these studies to larger fields.

Other beautiful experiments in Circuit QED have been realized, notably at Yale and at ETH in Zurich. For more details, and for a collection of papers on other experiments with superconducting qubits in quantum information, see the web pages of the groups at USBC, Yale, ETH and Saclay (CEA):
http://www.physics.ucsb.edu/~martinisgroup/ ; http://www.eng.yale.edu/rslab/

http://www.qudev.ethz.ch/; http://iramis.cea.fr/drecam/spec/Pres/Quantro/

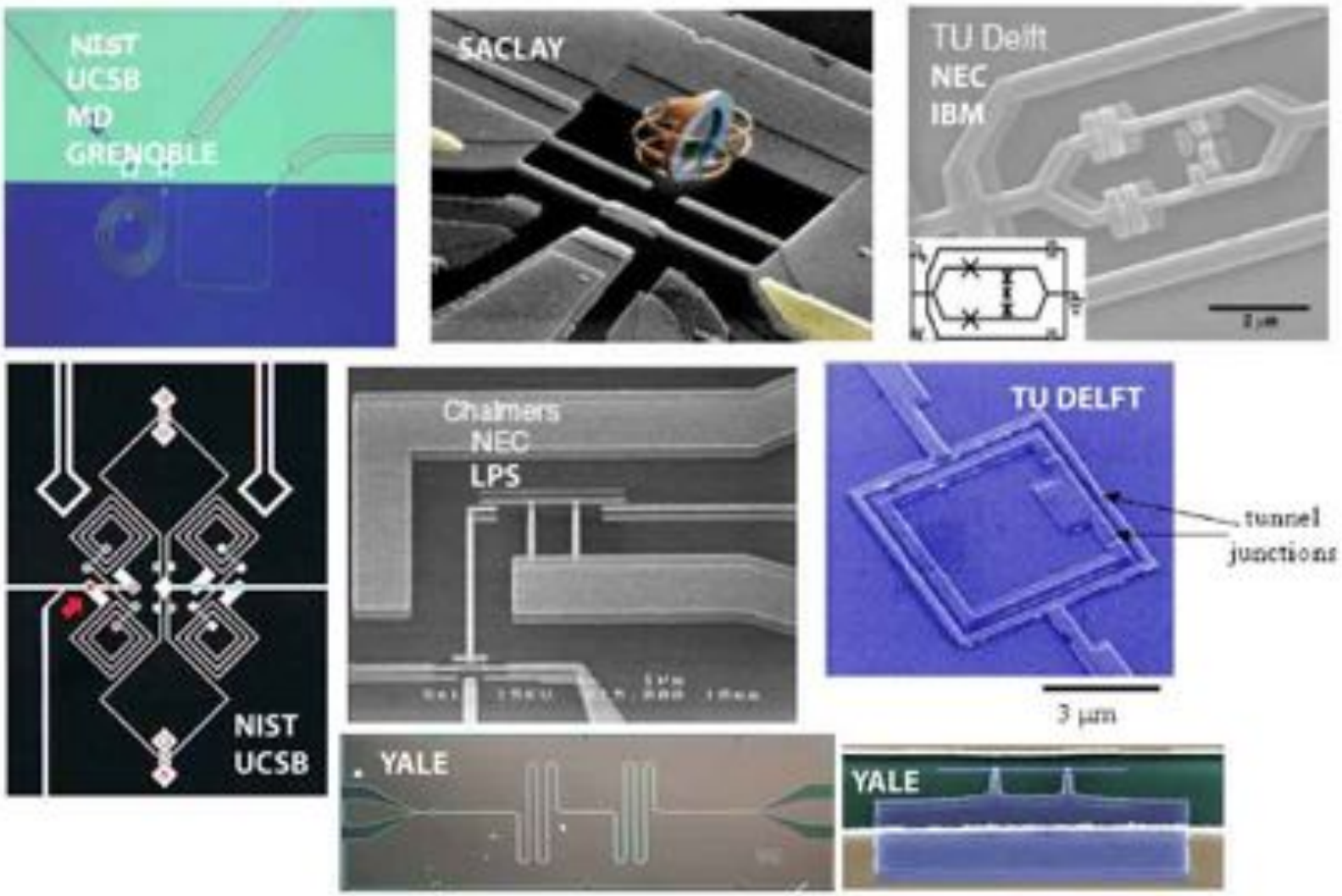

A zoo of superconducting qubits

(microphotographs of qubits realized in various labs, photo from website of the physics department at Rutgers University)

The ENS CQED group

Photo credit: M.Lebidinsky, CNRS

Suggested papers for the reports of QT5201E students

Cavity QED experiments:

J.M.Raimond, M.Brune and S.Haroche, "Colloquium: Manipulating quantum entanglement with atoms and photons in a cavity", Rev.Mod.Phys. 73, 565 (2001).

S. Gleyzes, S.Kuhr, C. Guerlin, J. Bernu, S. Deléglise, U. Busk Hoff, M. Brune, J-M.Raimond and S. Haroche, «Quantum jumps of light recording the birth and death of a photon in a cavity », Nature, 446, 297 (2007).

C.Guerlin, J.Bernu, S.Deléglise, C.Sayrin, S.Gleyzes, S.Kuhr, M.Brune, J-M.Raimond and S.Haroche "Progressive field-state collapse and quantum non-demolition photon counting", Nature, 448, 889 (2007).

S.Deléglise, I.Dotsenko, C.Sayrin, J.Bernu, M.Brune, J-M.Raimond and S.Haroche, "Reconstruction of non-classical cavity field states with snapshots of their decoherence", Nature, 455, 510 (2008).

C.Sayrin, I.Dotsenko, XX.Zhou, B.Peaudecerf, T.Rybarczyk, S.Gleyzes, P.Rouchon,M.Mirrahimi, H.Amini, M.Brune, J-M.Raimond and S.Haroche "Real-time quantum feedbackprepares and stabilizes photon number states", Nature 477, 73 (2011).

Circuit QED experiments:

.R.Schoelkopf & S.Girvin, Wiring-up quantum systems, Nature, **451**, 664 (2008)

•J.Clarke & F.Wilhelm, Superconducting quantum bits, Nature, **453**, 1031 (2008)

. Deterministic entanglement of photons in two superconducting microwave resonators H. Wang, Matteo Mariantoni, Radoslaw C. Bialczak, M. Lenander, Erik Lucero, M. Neeley, A. O'Connell, D. Sank, M. Weides, J. Wenner, T. Yamamoto, Y. Yin, J. Zhao, John M. Martinis, A. N. Cleland PRL 106, 060401 (2011).

. Synthesizing arbitrary quantum states in a superconducting resonator Max Hofheinz, H. Wang, M. Ansmann, Radoslaw C. Bialczak, Erik Lucero, M. Neeley, A. D. O'Connell, D. Sank, J. Wenner, John M. Martinis, A. N. Cleland Nature 459, 546-549 (2009)

. Generation of Fock states in a superconducting quantum circuit Max Hofheinz, E. M. Weig, M. Ansmann, Radoslaw C. Bialczak, Erik Lucero, M. Neeley, A. D. O'Connell, H. Wang, John M. Martinis, A. N. Cleland Nature 454, 310-314 (2008).

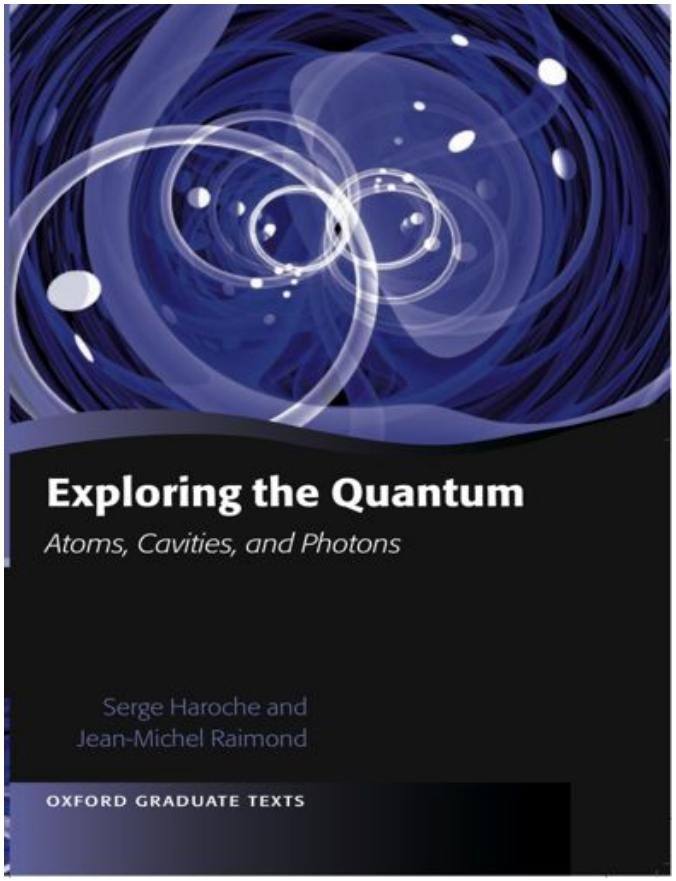

Exploring the Quantum

Atoms, cavities and Photons

S.Haroche and J-M.Raimond

Oxford University Press